PROCEEDINGS OF SCIENCE

Results of Iqueye, a single photon counting very high speed photometer at the ESO 3.5m NTT in 2009

C. Barbieri[1], **E. Verroi, P. Zoccarato, C. Germanà**
Department of Astronomy, University of Padua
Vicolo Osservatorio 3, 35122 Padova, Italy
E-mail: cesare.barbieri@unipd.it

G. Naletto, T. Occhipinti, I. Capraro
Department of Information Engineering
Via Gradenigo 6, 35100 Padova, Italy
E-mail: giampiero.naletto@unipd.it

M. Barbieri, L. Zampieri
INAF – Astrophysical Observatory of Padova
E-mail: mauro.barbieri@oapd.inaf.it

S. Gradari
CISAS, University of Padova, Italy
E-mail: serena.gradari@unipd.it

Iqueye is a single photon counting very high speed photometer built for the ESO 3.5m New Technology Telescope (NTT) in La Silla (Chile) as prototype of a 'quantum' photometer for the 42m European Extremely Large Telescope (E-ELT). The optics of Iqueye splits the telescope pupil into four portions, each feeding a Single Photon Avalanche Diode (SPAD) operated in Geiger mode. A first very successful run was performed in Jan 2009; both very faint and very bright stars were observed, demonstrating the high photometric quality of the instrument over a wide dynamic range. The first run allowed also to identify some opto-mechanical improvements, which have been implemented for a second run performed in Dec 2009. The present paper will describe the first version, the improvements implemented in the second one, and some of the obtained astronomical results both on optical pulsars and digital Hanbury Brown – Twiss Intensity Interferometry.

Keywords: high-speed photometry, extremely large telescopes, quantum optics, intensity interferometry, avalanche photodiodes

[1] Speaker

PoS(HTRA-IV)032

PROCEEDINGS OF SCIENCE

High Time Resolution Astrophysics IV - The Era of Extremely Large Telescopes-HTRA-IV
Agios Nikolaos, Crete, Greece
May 5-7 2010

1. Introduction

Astronomy has greatly expanded its frontiers, in particular by adding new spectral regions to those observable from the ground. Another frontier still exists, that of the shortest time intervals. Commonly available instruments rarely push their time tagging capability below the millisecond barrier. Modern technology, especially in the field of very fast photon counting detectors, gives means to overcome the presently achievable time resolution. To explore this possibility, we carried out the conceptual study of a very fast photometer, called QuantEYE [1] in the frame of the plan to instrument the ESO 100m OWL telescope. QuantEYE was in theory capable to determine the arrival times to better than 100 picoseconds, handling GHz photon counting rates. The OWL concept was superseded by the more affordable 42m Extremely Large telescope E-ELT, but our study maintained its validity. Given that the E-ELT is still several years in the future, we decided to acquire a sound experience with such unconventional instrumentation by building two prototypes, the first one for the Asiago 1.8m telescope (Aqueye [2]), the second one, Iqueye, for the 3.5m New Technology telescope (NTT) of ESO in La Silla (Chile). Both instruments are fixed-aperture photometers which collect the light within a field of view (FoV) of few arcseconds and focus it on single-photon diodes (SPADs) operated in Geiger mode [3]. The basic choices made for Aqueye were adopted also with Iqueye, but with noticeable improvements, as explained in Section 2 (see [4] and **[5]**). The experience gained by running the first version of Iqueye (Iqueye1) in January 2009, suggested the implementation of additional features, which will be described in Section 3. Some astronomical results obtained in January and December 2009 will be expounded in Section 4. Finally, Section 5 will provide a summary of our program and the description of possible future developments.

2. The first version of Iqueye (Iqueye1)

Using the experience gained with Aqueye, during 2008 we constructed another photometer (Iqueye1) for the 3.5m ESO NTT, which was brought to the telescope and successfully operated in January 2009. The same optical concept of splitting the pupil in 4 by means of a pyramid was retained, as shown in Fig. 1. At the *f*/11 focus of the NTT, a holed mirror diverts the field around the wanted target into a CCD camera, in order to facilitate its identification and centering. The light from the target object instead passes through the hole and is collected by a collimating refracting system. After the hole (which has a diameter of 5.4 arcsec), the light enters a 1:3.25 reduction optics, where filters can be inserted in the parallel beam (the two wheels contain 7+7 filters, plus two clear positions). The beam is then focused on a selectable pin-hole (200, 300 and 500 micrometers, respectively). These pinholes act as field stops, and their size allows the selection of three different FOVs. Taking in account the 5.36 arcsec/mm nominal NTT scale factor at the Nasmyth focus, the diameters of the selectable FoVs are 3.5, 5.2, and 8.7 arcsec, respectively. After the pinhole, the beam diverges to the 4- faces pyramid, whose tip coincides with the center of the secondary mirror shadow. This optical element divides the telescope pupil into four equal portions, and sends the light from each sub-pupil

along four perpendicular arms. Along each arm, the sub-pupil light is first collimated and then refocused by a suitable lens system, which further (de)magnifies the image by an additional 1/3.5 factor, over the SPAD. Therefore, the SPAD circular sensitive area of 100 μm diameter, nominally defines a FoV of 6.1 arcsec.

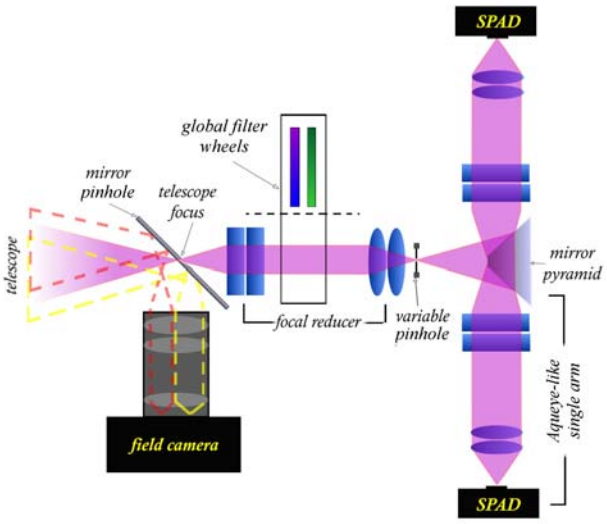

Figure 1: The conceptual scheme of Iqueye1, from the NTT focus to the 4 SPADs.

The smallest pinhole acts as a 3.5 arcsec field stop. This pinhole can be selected when it is necessary to reduce as much as possible the background around the target, as when observing a pulsar embedded in a nebula.

However, if the seeing or telescope oscillations (e.g. due to wind buffeting) deteriorate the stellar profile to more than 1.0 arcsec FWHM, fluctuations of the signal of the order of few percent are noticed. These fluctuations are not important when observing a pulsar with a precise time signature, but limit the precision of conventional photometry. The intermediate 5.2 arcsec pinhole is more closely matched to both entrance aperture, detector size and average seeing values. Moreover, it accounts for the small spot broadening caused by system residual aberrations. This is therefore the pinhole selected for the standard operating conditions. Finally, the larger 8.7 arcsec pinhole is used mainly for alignment and/or calibration purposes.

The optical requirements of Iqueye are not really stringent, since it behaves like a focal reducer. In addition, splitting the beam into 4 parts causes a reduction of a factor 4 in the optical invariant, lowering the speed and aberrations along each arm, and thus simplifying the optical design. Because of this simplification, it was possible to build the optical train of Iqueye1 using only commercial spherical lenses, yet still obtaining good performance: by ray-tracing, the energy encircled in the SPAD sensitive area was 93% for a 5 arcsec diameter uniformly illuminated source. However, the optical design showed that improvements were possible, because the percentage of light focused on the detector was not much greater than 97% even in the case of a point source. The main culprit was the residual aberration of commercial lenses; an optimized lens design would allow us to collect a percentage of radiant energy greater than 99%. This amelioration was indeed implemented in the second version of Iqueye, Iqueye2, as described in Section 3.

As detectors for Iqueye, we selected second-generation SPADs produced by MPD Italy. With respect to the SPADs used in Aqueye, the active area increased from 50 to 100 micrometer diameter, maintaining the same timing precision and actually lowering the dark counts to less than 50 Hz. The benefits of SPADs are numerous: in contrast to other photon counting detectors, they can tolerate full daylight also when powered; their quantum efficiency approaches 60% at 550 nm, as measured in the laboratory of the Catania Observatory [6]. They are thermoelectrically regulated at a nominal temperature of −10°C to maintain low the dark count rate; they have an almost flat BK7 window coated with high efficiency anti-reflection coating which does not alter the optical quality of the focused beam, and divides the active area from the ambient, allowing safe operations and avoiding condensation onto the sensitive area; the integrated timing circuit provides an extremely accurate signal, providing a time tag jitter of the order of 35 ps; they are packaged in a robust box that allows easy handling, and their price is reasonably low. The disadvantages are a typical after-pulsing probability of around 1%, a linear count rate up to only 2 MHz when using the NIM output (the count rate linearity is as high as 12 MHz with the TTL output, which however has a less accurate time-definition capability), and finally a dead time of ≈75 ns after each detected event. The dead time limits the dynamics to higher rates when observing a bright source, and is particularly severe for quantum applications, where photon statistics must be measured. Another advantage of splitting the beam into four parts by means of a pyramid is to alleviate the effect of this 75 ns dead time: the parallelism between the sub-pupils, and the consequent use of four detectors, partially overcomes this problem. Because of the statistical distribution of events over the four detectors, many events that would be otherwise lost are recovered.

The mechanical structure of Iqueye and its interface to the conical flange of the NTT (see Fig. 2) have been designed and built by the firm Tomelleri Italy. Mounting and aligning of the optics and detectors were performed in the optical laboratory of the Department of Information Engineering (see Fig. 3).

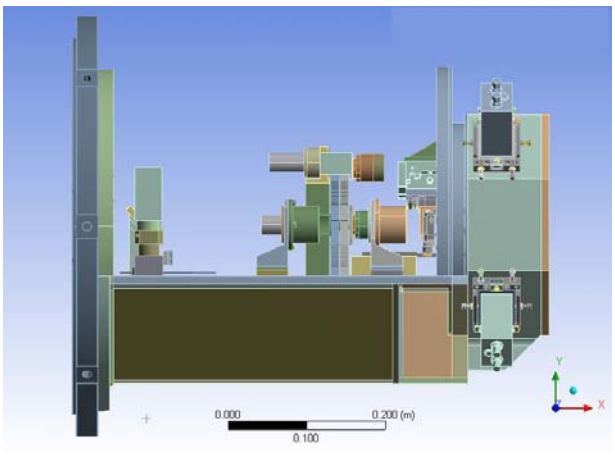

Figure 2: The mechanical design of Iqueye.

Figure 3: Left: Iqueye1 on the optical bench at the Department of Information Engineering. Right: the rear side of Iqueye1, with the 4 SPADs fed by the central pyramid.

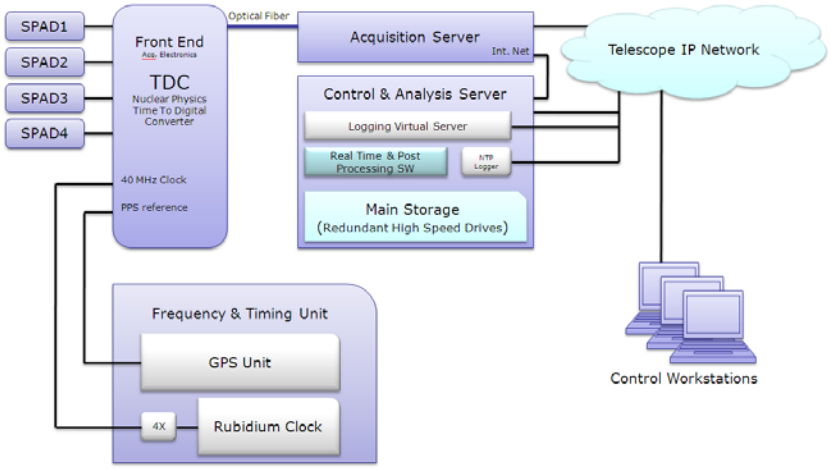

Figure 4: Iqueye Data Acquisition System from the SPAD's output to the CAEN TD board to the time and frequency unit ITFU, to storage unit and control.

The Iqueye Data Acquisition System (IDAS, see Fig. 4) collects the pulses produced by each SPAD for every detected photon, assigns a very accurate absolute time tag to each event, and stores the time tags in the external memory. Each of the 4 NIM signals is transferred from the SPADs, by means of calibrated equal electrical length coaxial cables (provided and certified by MPD) to ensure the same electrical delay, to one of the input channels of a time to digital converter (TDC) board (CAEN V1290N), originally developed for high energy physics applications. This TDC board is nominally able to time-tag the voltage pulses on its inputs with a 24.4 ps time resolution, obtained by means of a 40 MHz internal oscillator whose frequency is multiplied by 1024 by means of a phase locked loop (PLL) and a delay locked loop (DLL), providing a 40 GHz clock. Requirements on timing accuracy are very strict, namely IDAS must produce an absolute, UTC referenced time tag for each detected photons with a rms accuracy of the order of 500 ps for at least one hour of continuous operation, coping with count rates ranging from few tens of Hz up to tens of MHz. As already mentioned, the SPAD has two

different outputs: a TTL one, which can sustain count rates as high as 12 MHz in the linear regime, with about 250 ps timing jitter, and a NIM one, which has a maximum linear count rate of about 2 MHz, but a much better 35 ps typical timing accuracy. Since Iqueye was designed to reach a rms time tagging resolution of the order of 100 ps, the NIM output was adopted as a baseline, notwithstanding the lower possible maximum count rate. The TTL output can be used in parallel, mainly for control purposes. Unfortunately, the quality of the internal oscillator in the CAEN board is insufficient to satisfy the extremely severe stability requirement of our applications, for which it is necessary to obtain simultaneously both the short-term stability typical of a quartz oscillator and the long-term one assured by a primary time reference.

The selection of a hydrogen-maser as primary time reference was not possible, because of its high cost and difficulty to operate it at the NTT. To obtain a nearly optimal and affordable performance for the Iqueye time and frequency unit (ITFU), we selected a combination of a rubidium oscillator, a GPS receiver, and a post-processing algorithm. ITFU (shown in Fig. 5), is based on the concept of correcting the long-term drift of the rubidium oscillator (a Stanford Research System FS275), which ensures good stability for medium lengths of time ($<10^4$ s), by means of a post-processing algorithm that uses the pulse-per-second (PPS) signal provided by GPS receiver (a mini-T Trimble) [7].

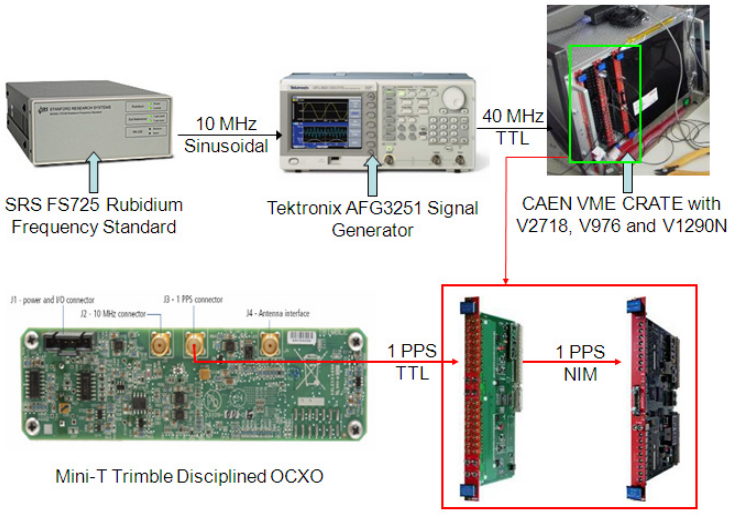

Figure 5: Block diagram of the Iqueye time and frequency unit (ITFU), which provides the frequency standard to the experiment. OCXO is an acronym for Oven-Controlled Crystal Oscillator.

The rubidium oscillator produces a 10 MHz sinusoidal signal, converted to a 40 MHz TTL signal by means of a frequency multiplication by a Tektronics AFG3251 pulse generator and a signal generator. The 40 MHz TTL signal is inputted to the CAEN board as its frequency standard, disabling the on-board clock. The rubidium oscillates in free-running mode, namely not disciplined by an external reference, because tests performed at the Astronomical Observatory of Cagliari using a primary standard Caesium clock as reference, showed that this solution would improve the phase noise. Furthermore, these tests showed that the rubidium

accumulates a phase drift of approximately 65 ns after half an hour, and 360 ns after two hours [8].

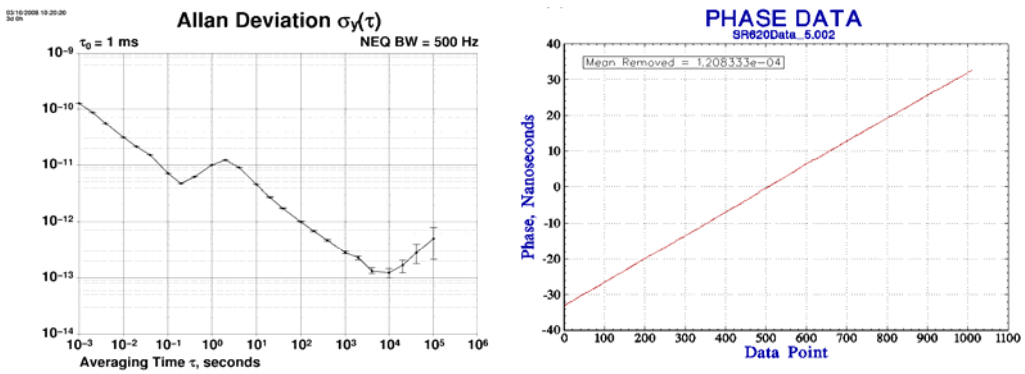

Figure 6: Characterization of the Allan deviation (on the left) and phase drift (on the right) of the SRS FS725 rubidium frequency standard in free running at the Time & Frequency Laboratory of the Astronomical Observatory of Cagliari.

By removing such drift, only a residual stochastic phase error remains, whose rms value is lower than 50 ps for a duration of more than 1000 s (see for example Fig. 8). The Allan variance has a minimum corresponding to 3×10^{-13} after 10^4 s (see Fig. 7).

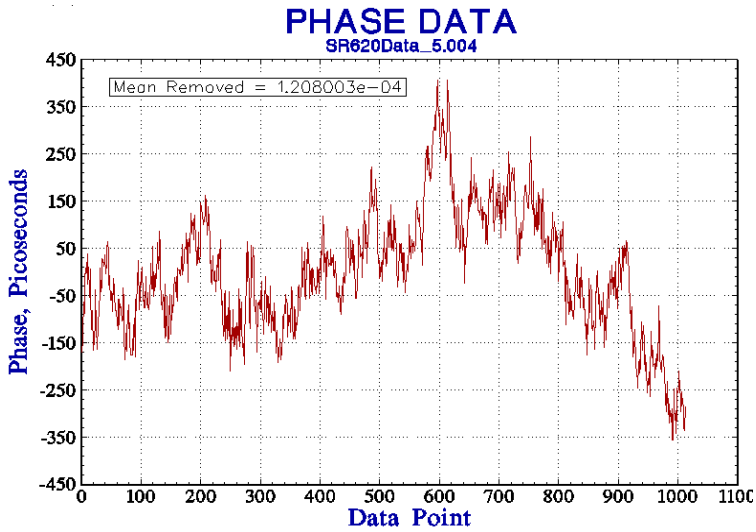

Figure 7: Differences between an ideal PPS signal and the real PPS signal corrected for rubidium phase drift. The abscissa spans over 1000 s, the ordinate between –450 to + 450 ps.

By summing the rms time errors in the SPADs (35 ps), those in the electronics chain (50 ps), and the residual phase errors (50 ps for one hour of observation) to the internal sampling discretization (24.4 ps), a total rms time error of approximately 100 ps is obtained, which satisfies the design requirements. This is the level of relative rms time accuracy that ITFU insures for one-hour long observations. The PPS's produced by the GPS receiver are used both to remove the linear drift and to obtain the UTC synchronization while operating at the

telescope. These PPSs are given to the CAEN board via a TTL/NIM converter as input pulses on a fifth channel, and are processed in the same way as photon pulses from the 4 SPADs. Finally, the UTC corrected time tags are made available for further processing.

The start signal of the acquisition process is provided by the main PC, whose system clock is disciplined by the Network Time Protocol with a typical uncertainty of few milliseconds. To lower this uncertainty, the true start of the acquisition is given by the first PPS encountered in the data string, having an rms uncertainty of approximately ±25 ns typically associated with a single frequency GPS receiver. Thanks to the linear drift interpolation, the error associated with the starting time decreases with the number of acquired PPS's: after one hour of observation this error decreases to 0.4 ns rms. In summary, recalling the 100 ps relative time accuracy for an acquisition of one hour, an absolute rms time accuracy with respect to UTC of better than 0.5 ns is obtained.

A limitation of the TDC board is that it returns a 21-bit time-tag value. Given the 24.4 ps time digitization, the longest unambiguous time interval is only $\Delta t = 51.2$ μs, while all times longer than this interval have an initial phase $N\Delta t$, where N is an integer to be determined. To realize this so-called "de-rollover" process, the TDC board is fed with an external 20 kHz reference pulse, which allows to determine the value of N and recover the initial phase.

The overall system was designed with a modular approach. The TDC board is equipped with 16 inputs, of which only six are used at present, so that a further expansion of the number of detectors is possible with no need to upgrade the IDAS. Moreover, the TDC board is lodged inside a standard crate, which can host additional boards all connected to the same VME bus. In practice, other TDC boards can be added, if necessary, with no need to modify the present system.

All the electronics equipments were mounted into a standard 19'' rack, grouping together the acquisition system, the time and frequency reference, the control for the motors, the processing units. The rack is placed inside the NTT Nasmyth B focus room, and is connected to the IP network of NTT, so that the instrument can be commanded remotely from the control room, as shown in Fig. 9. Two high performance servers are mounted inside the rack. The first server is connected via a short fiber to the VME bus, and to the second server where all the acquired scientific are were stored. The second unit has the task to coordinate the overall Iqueye instrument, and is connected to each electronics subsystem (see again Fig. 5).

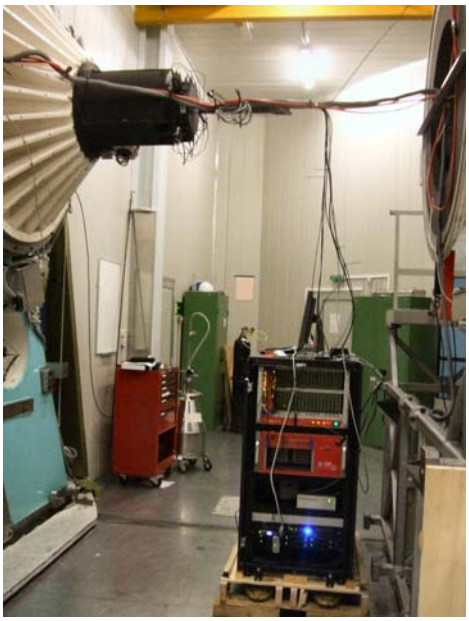

Figure 8: Iqueye1 mounted on the conical interface of the NTT Nasmyth B room. The cables to the acquisition and control electronics were so mounted to allow the rotation of the telescope field of view.

The storage capability is approximately 2 Terabytes, and all the data are recorded in a 6 SATA disks raid6 configuration, in order to assure both redundancy and speed in accessing the database. Moreover, a virtual server was configured inside the second one for controlling all the subsystems data and functionalities. A multitasking software program in Java language has been developed, connecting each instrument subsystem, and displaying several real time statistical analysis of the data acquired during the observations. Moreover, this software is able to read and store the images of the stellar field around the wanted object acquired by the field camera. These images can be used for a a-posteriori analysis of guiding errors and sky conditions.

3.The Improved Iqueye (Iqueye2)

The very successful run of January 2009 suggested some additions to Iqueye1, which were implemented in time for the December 2009 run. The main additions are listed in the following.

The insertion of a filter wheel in each arm, in order to perform multicolour simultaneous photometry, as shown in Fig. 9. Each wheel can hold 4 filters plus an empty hole, it is motorized and remotely controlled.

The spherical commercial lenses of the doublets in front of the SPAD's have been replaced by other optimized custom designed spherical lenses, in order to ameliorate the concentration of light inside the active area of the SPAD. The achieved result is that more than 99% of the polychromatic encircled energy from a 5 arcsec uniformly illuminated extended source is concentrated inside the pixel. Fig. 10 shows the encircled energy in the case of a 2 arcsec uniformly illuminated source.

A fiber fed fifth SPAD has been added on the focal plane of NTT. The entrance lens of 5 mm clear aperture diameter defines a FoV of approximately 8 arcsecs (of which only the central 4 are unvignetted). The SPAD sees therefore a small portion of the sky, and the corresponding signal can be used to monitor transparency variations and behavior of the overall electronic chain.

The cumbersome 6 hard drives server, and the virtual machine, were removed, installing in their place a new compact server equipped with Windows Server 2003. This unit has 2.5 Terabytes storage capabilities assured by 2 SATA HD. At the end of the observations, the data are copied on a 2 Terabytes external USB HD for subsequent processing.

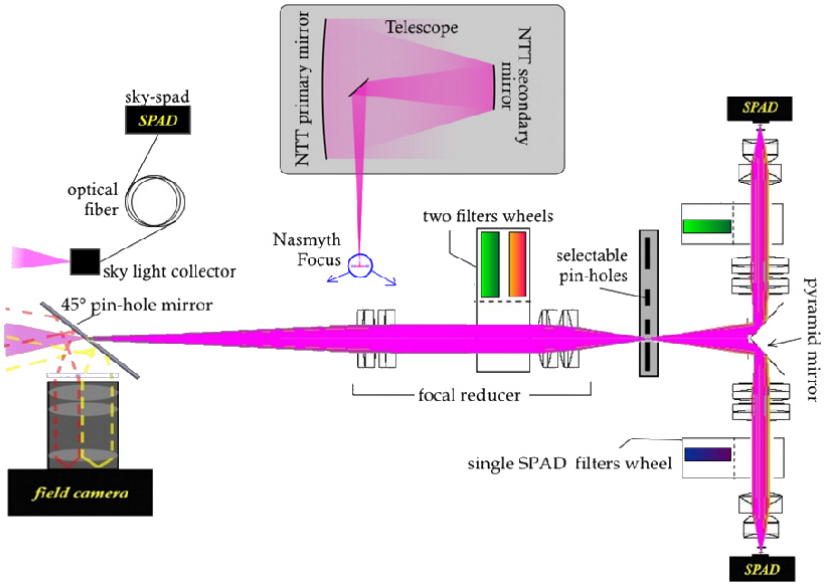

Figure 10: The conceptual scheme of the second version of Iqueye, with the addition of a fifth SPAD for sky control and a filter wheel in each arm.

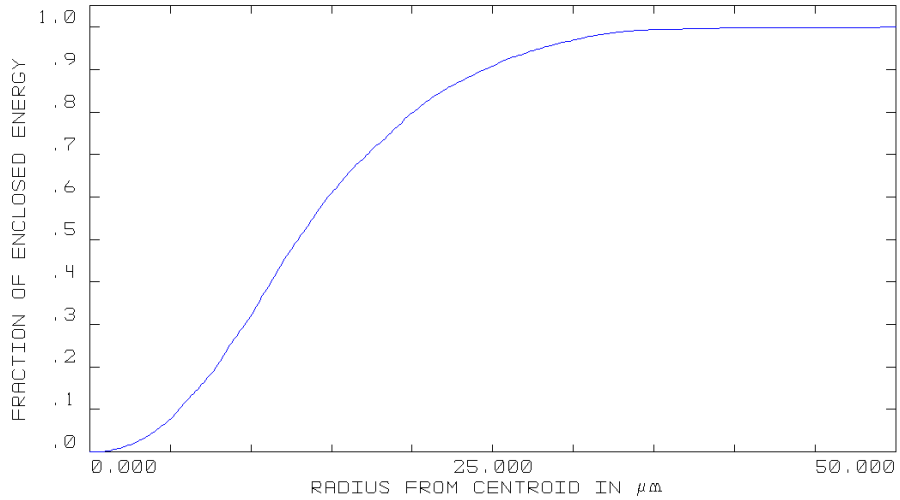

Figure 91: Polychromatic encircled energy from a uniformly illuminated 2 arcsec extended source: 99.9% of the energy is encircled within a radius of 43 μm.

4.Astronomical results

The global efficiency of the system for astronomical observations has been estimated by taking into account the three reflections of NTT mirrors, the reflection at the pyramid, the nominal transmission of all the lenses, and the detector quantum efficiency. The result is shown in Fig. 11, together with the expected sensitivity when using the three B, V, and R wide-band filters. It can be seen that the global sensitivity curve is dominated by the SPAD efficiency, reaching a peak of more than 33% at 550 nm. From this curve, it is also possible to evaluate the expected signal-to-noise ratio (SNR) as a function of the target magnitude.

As an example, Fig. 12 shows the calculated exposure times needed to achieve the required SNR for a given exposure time, in the V-band, per single SPAD, assuming a source at zenith, no moon light, a sky brightness of 21.9 mag/arcsec (data for La Silla were taken from: http://www.vt-2004.org/gen-fac/pubs/astclim/lasilla/index.html), a collected FoV of 3 arcsec, and a detector dark count rate of 50 c/s. At the faintest magnitudes, Iqueye SNR is limited by the detector dark count and not by the night sky.

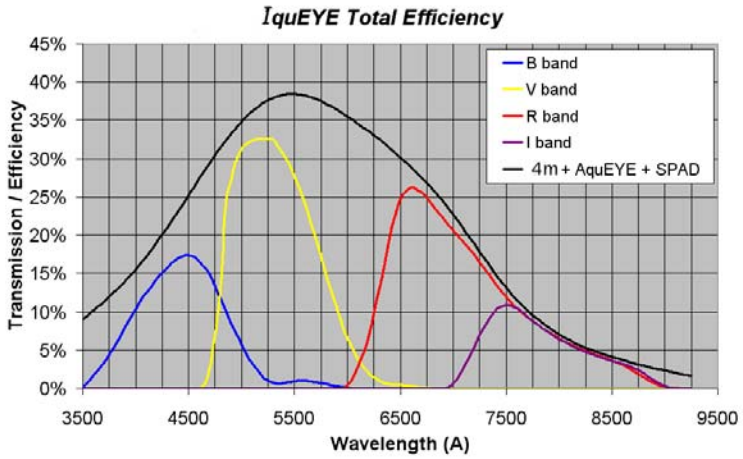

Figure 102: The global efficiency of the system.

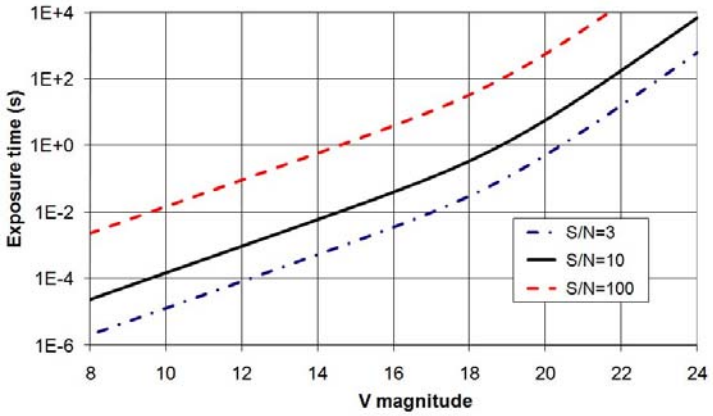

Figure 113: The calculated exposure time to reach a wanted SNR in the V band.

Table 1 gives the list of available filters in the entrance wheels, and Table 2 of those in the individual arms (this latter complement can be easily modified on site). The main characteristics describing the performance of Iqueye applied to NTT are summarized in Table 3.

Table 1: Main characteristics of the filters/polarizers available on the two entrance filter wheels.

Position	**Wheel 1**	**Peak (nm) / FWHM (nm)**	**Wheel 2**	**Peak (nm) / FWHM (nm)**
1	B	433/101	Neutral 1	–
2	V	531/82	Neutral 3	–
3	R	747/234	HeII	468/2
4	IR	817/179	[OI]	630/2
5	[OIII]	501/1.31	Pol Vis	Peak extinction ratio > 1:1000
6	Hα	656/3	Pol UV	Peak extinction ratio > 1:100 000
7	Shutter	–	Neutral 2	–
8	clear	–	clear	–

Table 2: Filters on the individual arm.

Position	**Filter**
Spad 1	B
Spad 2	V
Spad 3	R
Spad 4	empty

Table 3: Overall characteristics of Iqueye2

system sensitivity	photon counting
relative time accuracy	100 ps (for 1 h of continuous observation)
absolute time accuracy	500 ps (for 1 h of continuous observation)
dark count rate	<100 Hz per SPAD
maximum total count rate	8 MHz
dynamic range	>40 dB
limiting magnitude	V = 24 with 2 h exposure time and S/N = 10
effective field of view	(selectable) 3.5, 5.2, or 6.1 arcsec
operative spectral range	$\Delta\lambda$ = [350, 925] nm (see Table 1 and Table 2 for filter details)
system total efficiency	33% (peak @ 550 nm) 18% (average over $\Delta\lambda$ = [350, 925] nm spectral range)

We performed our observations at the NTT on 14-19 January and then on December 12-18, 2009, operating Iqueye across its entire range of count rates, from extremely faint to very bright sources. The capability of our apparatus to time-tag photons with extremely accurate precision over a very wide dynamic range was demonstrated convincingly.

The data obtained on the pulsar of the Crab Nebula and on the pulsar in Vela, illustrate the capabilities of Iqueye in high speed photometry. Fig. 13 shows a string of individual pulses from the 33 ms Crab pulsar, with the counts binned in 1.0 ms time bins, namely at 1/33 of the pulsar period. Fig. 14 shows the power spectrum of the signal obtained from the 80 ms Vela pulsar, approximately 10 times fainter than the Crab. Individual pulses cannot be obtained, but the Fourier transform clearly evidences the strong expected periodicity in the signal. These cases are interesting also because they show the ability of Iqueye to identify the signature of a periodic phenomenon in a much stronger background due to the surrounding nebulae.

Another interesting application was the attempt to perform intensity interferometry [9] over the four sub-apertures of the NTT. This case is discussed in detail in [10] so we refer to this paper for further information.

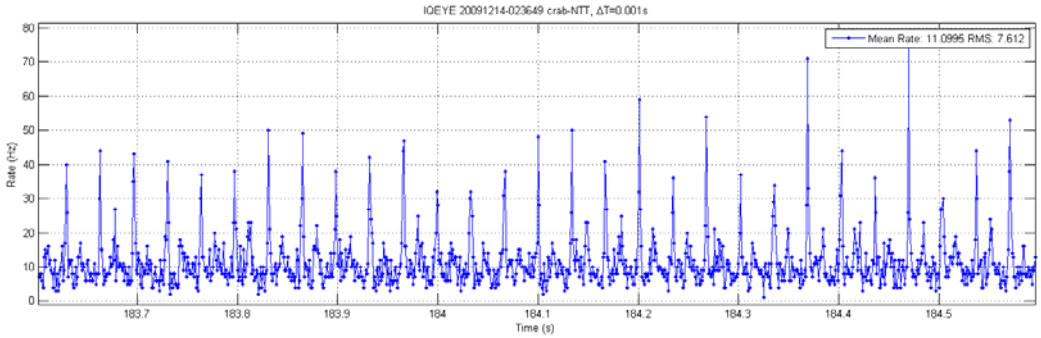

Figure 124: Individual pulses from the Crab Nebula pulsar obtained in Dec. 2009 with Iqueye2.

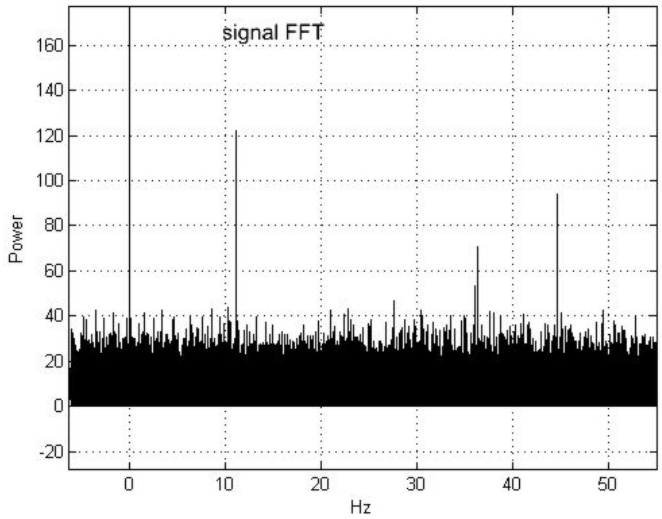

Figure 135: Power spectrum of the signal from the 80 ms Vela pulsar obtained in Dec. 2009 with Iqueye2.

5.Second order correlation results with Iqueye

This section illustrates how quantum astronomy can be achieved by the calculation of $g^{(2)}$, i.e., the second order correlation function (see Ref. [2], [8]; [9]) using the present technology of Iqueye. In particular, we verified the capability of Iqueye to perform the measurement of $g^{(2)}(d)$ as a function of the relative distance d of the collecting apertures, thus confirming its effectiveness as an intensity interferometer.

HBTII is performed by calculating the second order correlation of the intensity data $I(\mathbf{r},t)$ given by the formula:

$$g^{(2)}(\boldsymbol{d},\tau) = \frac{\langle I(\mathbf{r}_1,t_1)I(\mathbf{r}_2,t_2)\rangle}{\langle I(\mathbf{r}_1,t_1)\rangle\langle I(\mathbf{r}_2,t_2)\rangle} \qquad (1)$$

where $\boldsymbol{d} = \mathbf{r}_2 - \mathbf{r}_1$ is the baseline between two collectors and $\tau = t_2 - t_1$ is the time-shift between photons. In particular, HBTII applies to the case $\tau = 0$ and $\boldsymbol{d} \neq 0$, whereas when $\tau \neq 0$ and $\boldsymbol{d} = 0$ correlation spectroscopy is performed. In both cases, when considering a photon counting device such as Iqueye, the signal to noise ratio *S/N* is given by :

$$(S/N)_{RMS} = \frac{1}{2}(N_1 N_2)^{1/2}\tau_0\left|\gamma(\boldsymbol{d},\tau)\right|^2\left(T_0/2\Delta t\right)^{1/2} \qquad (2)$$

where N_1 and N_2 are the number of collected photons in the two collectors respectively, τ_0 is the coherence time of the radiation, γ is the complex degree of coherence, T_0 the exposure time and Δt is the coincidence windows used to perform the measurement [7].

The following figure reports a simulation of *S/N* on an Iqueye-like instrument attached to several telescopes, in the visible, through a bandpass of 1 nm, in 1 h counting time. For reference, the lower curve shows the performance of the Narrabri experiment, with two 6.5 meter apertures. The Iqueye-like curves saturate at high fluxes due to SPADs dead time. As can be seen from the curve immediately above Narrabri's, a pair of 1.8 m class apertures (corresponding to the 3.5 m NTT with the pupil divided in four), would provide in one hour of data taking a *S/N* ratio ten times better than possible at Narrabri. In other words, stars down to the fifth visual magnitude can be measured with a fair *S/N* ratio. The other curves show the expected results with the gradual increase of the size of the apertures, from two 4 m apertures (two sub-pupils of the VLT or Keck telescopes) to two fully illuminated VLT of Keck telescopes to two 20 m apertures (two subpupils of the 42 m E-ELT). The increase in the number of SPADS parallels the increase in the photon flux, in order to cope with the 75 ns dead time limitation.

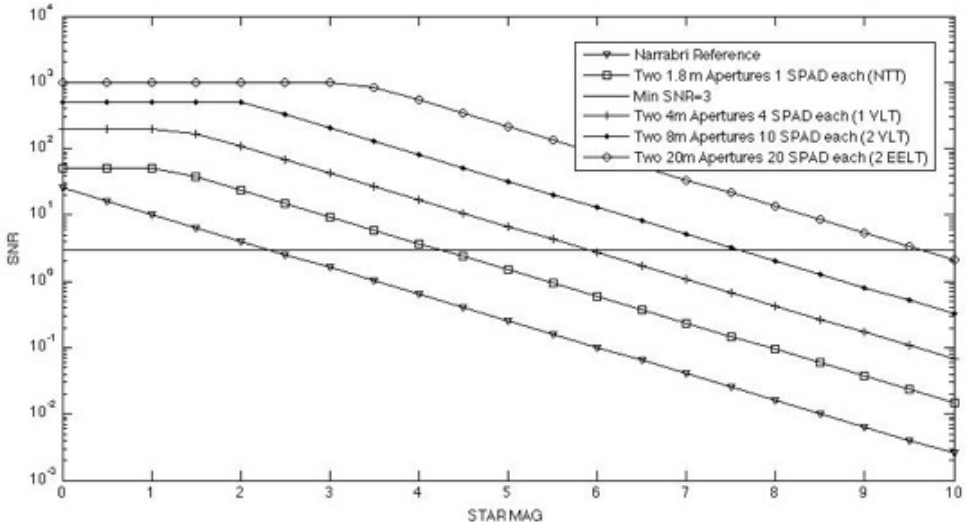

Figure 16: SNR of an Iqueye like instrument attached to different telescopes, in 1 h data acquisition time, in the visible, over a bandpass of 1 nm.

From the astrophysical point of view, these capabilities would mean that two fully illuminated VLT or Keck telescopes would resolve in blue and visible wavelengths essentially all naked eye stars in the Main Sequence, and not only supergiants in red light, as generally possible with Michelson-type interferometers. Moreover, at least one active galaxy (NGC 1068) could be resolved using its bright emission lines.

The present electronics of Iqueye comes short of the results indicated in Fig. 2 because of the 8 MHz limitation in the overall data stream, but this shortcoming is not intrinsic to the device. Given more resources, present technology can raise the photon rate by at least a factor of four, as discussed in the last section of this paper. Nevertheless, even with such limitation, Iqueye produces a huge amount of data: an hour of observation on a bright star produces approximately 100 GB of data. In order to handle the correlation of such long string of time tags an *ad hoc* software correlator has been implemented, which works directly on the time tags t_i using a different approach with respect to standard calculation of a correlation function, as explained in the following.

5.1 The Iqueye software correlator

In usual methods, correlation functions are calculated by means of FFT algorithms, passing from time to frequency domain. This method is normally very fast and works very well with "continuous" functions. In the Iqueye case, however, the function to be correlated is not a continuous one: the instrument generates a sequence of many zero's (namely, the time bins in which no event has been detected), with just a few one's corresponding to the time bins in which one event has been detected. For this type of "sparse" discontinuous functions, the FFT algorithm is not so well performing, and a different way of calculating the correlation function has to be used.

It is important to understand the type of calculation necessary in this specific application. To perform HBTII, the second order correlation function has to be calculated for two different positions at the same instant. In practice, one has to calculate equation (1) when $t_1 = t_2 = 0$:

$$g^{(2)}(\boldsymbol{d},0) = \frac{\langle I(\boldsymbol{r}_1,0) I(\boldsymbol{r}_2,0) \rangle}{\langle I(\boldsymbol{r}_1,0) \rangle \langle I(\boldsymbol{r}_2,0) \rangle} \tag{3}$$

For Iqueye, this procedure amounts to calculate the number of "coincidences" on the output signal from two different SPADs coupled to two different sub-pupils of the NTT at a relative distance d: here "coincidence" means to have two events, one per SPAD, detected within the same time bin. In terms of the classical correlation function, this corresponds to calculate the correlation for just one value, namely at zero delay time. Obviously, the "zero" is not a single point, as it would be with a continuous function, but has a time extension given by the considered time bin. This time bin can be chosen as small as the actual time "unit" given by the TDC board (24.41 ps) or, more realistically using a larger value obtained by binning together by software some time "units", for instance a value which includes also the instrumental error. Since Iqueye's relative time accuracy is of the order of 100 ps, we can assume as a reasonable time bin (coincidence window, Δt) at least twice this value, that is 200 ps. In our numerical experiments therefore we choose a time bin ten times larger than the time "unit", namely 244.1 picoseconds.

Since our specific problem is reduced to the calculation of the correlation function at one single value, standard algorithms are actually largely oversized, because they usually return a number of correlation values as high as the number of elements of the input arrays. In addition, we have to consider the huge number of elements of the input arrays provided by an Iqueye-like instrument. As already said, the functions we have to correlate are extremely long arrays of bits, one per each time unit: "0" when there is no detected event, "1" when an event is detected at that particular time unit. So, for example, sampling one hour of observations using a 244.1 ps time bin (10 time units) corresponds to have arrays with about 1.5×10^{13} elements: each of the files to be correlated would have a size of about 1.9 TB. Standard correlation algorithms would need an enormous amount of mass memory; in addition, as just mentioned, the result would have a huge amount of useless information, at least for this application, since only one out of the 1.5×10^{13} data point would be utilized. So, these algorithms are definitely not suitable for this application, and approaches different from the standard ones have to be found.

A first algorithm we envisaged as alternative to the classical ones was to realize a "single point correlation", namely an algorithm able to calculate the correlation directly at the zero time delay value of interest. The basic idea was to time shift one data set with respect to the other for a time interval equal to the coincidence window, and to calculate the coincidences. For example, in the case of a coincidence window of 244.1 ps, this would have implied: a) to realize 10 time shifts of one time unit each; b) to count the overlapped events, that is the events happening at the same time unit, for each time shift; c) then summing all these overlapped events. This sum would be the sought-for correlation value. However, also this algorithm would not solve the major problem of dealing with huge input arrays: in fact, the time units in one hour observation are of the order of 10^{14}, leading to input data set files of the order of 19 TB.

In a second attempt, we considered the method developed by Beck [10], who explicitly considers the case of detectors affected by dead-time problems such as our SPADs.

The value of a modified correlation function $G^{(2)}(d,0)$ is computed by means of the expression:

$$G^{(2)}(d,0) = N_{AB}\Delta T / (N_A N_B \Delta t), \quad (4)$$

where N_A and N_B are the total counts on detectors A and B respectively, and N_{AB} is the number of coincidences, that is the number of simultaneous event detections in A and B within a coincidence window Δt during an observation time ΔT. Determining the N_A and N_B values is straightforward, but this is not the case for N_{AB}. To calculate this latter value, we took advantage of the fact that the actual number of detected events is much smaller than the number of time units. For example, in the case of the observation of the bright star ζ Ori described in the following, which lasted 1 hour and 8 minutes (1.7×10^{14} time units), approximately 2×10^{10} photons were detected. So, storing the event time tags (28 bits each, plus some housekeeping data) is much more convenient: all the time tags of this observation were stored in 7771 files each of 10 MB, for a total of 78 GB, instead of the 21 TB needed to store all the time units.

Calculating the correlation of the time tags is now fairly simple: indicating with t_i the time tags of the events detected on one SPAD, and with t_j' the time tags of the events detected on the other SPAD, it is sufficient to increase by one the value of the correlation function at the time tag differences $t_j' - t_i$ ($t_j' > t_i$) for all the i,j events. The algorithm actually allows to calculate the correlation function for all time delays. However, in this specific case where we are interested in knowing only the value of the correlation function at zero, it is possible to apply the restriction $t_j' - t_i < \Delta t$, so greatly minimizing the needed calculations. A schematic view of the way of working of this algorithm is shown in Figure 2.

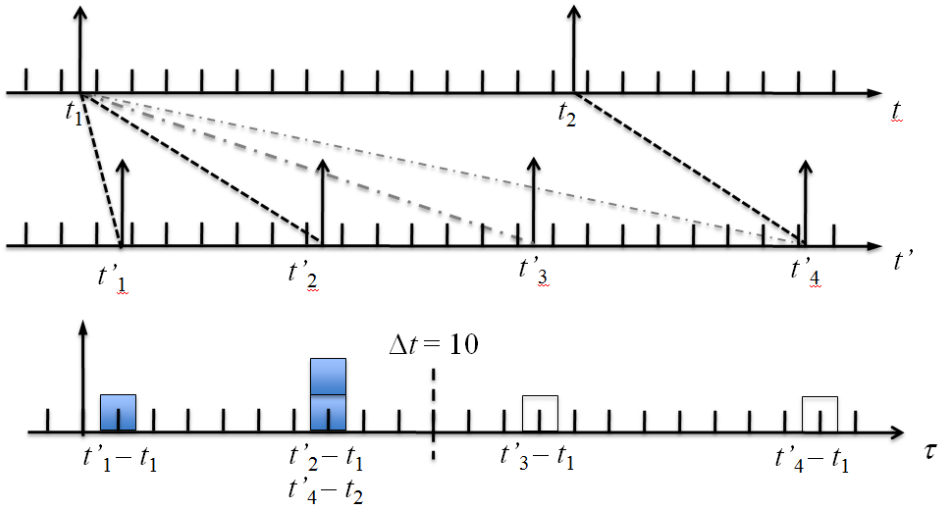

Figure 17: The software correlator works directly on the photon time tags, building the correlation step by step. Top: the two photon streams are shown along the two temporal axes t and t'. Bottom: the correlation at zero delay is calculated as the sum of the "coincidences" within the same coincidence window Δt (in this case considered to be equal to 10 time units). In the case in the figure, the t_1 event has two coincidences on the t' axis; the t'_3 and t'_4 events on

axis *t'* do not coincide with t_1 since they happen after a time interval longer than the coincidence window; however, the event at t'_4 is coincident with the t_2 event.

This approach has significant advantages with respect to the other possible approaches described above. First, it is optimized for this specific application, that is for the cases in which the function to be correlated is a sequence of sparse single events: this allows to have a result fitting to the actual needs, and not an oversized result which includes a great amount of not useful information. Second, it works on a smaller data set, since it uses time tags and does not require a binned intensity string: this allows to use standard computers (even if the whole data set usually has to be divided in a number of smaller data subsets) to perform the calculation of the correlation in a reasonable amount of time. Third, it is fast, because the possibility of restricting the coincidence windows allows to skip a great amount of calculation, optimizing the calculation time. Fourth, the number of computations is of order O(N), not O(N^2); even increasing the photon rate by say a factor of 10, the computing time would remain quite affordable even without supercomputers.

It is also worth to mention here the great advantage of using a software correlator with respect to a hardware one, as was originally done by Hanbury-Brown and Twiss. With a hardware correlator there is no possibility of storing the data, and no capability of doing any post-processing analysis; so, each acquisition gives a single result, independent of the capability of recovering possible errors in the setup, or of reconfiguring the parameter of analysis (e.g. to change the coincidence window). These are great limitations that are overcome by means of this software correlator.

The algorithm has been implemented as described in Ref. [11]. Even if any size of coincidence window Δt can in principle be selected, a further optimization has been realized by selecting coincidence windows equal to 24.41×10^N ps, where N is a non-negative integer: in this cases the computation time is minimized. As input, this routine needs the files that collect the time tags; the size of these data files remains large, however the algorithm performs the calculation in a reasonable time, even without the use of supercomputers, as shown in the following subsection.

5.2 Application of the software correlator to the bright star Zeta Ori

As an example of application of the method, we consider the data collected on the bright star ζ Ori (HD 37743, V = 1.8, SpT = O9.5Ib, with emission lines). The star was observed on January 21st, 2009 at UTC (start) 01h06m24s for 1h8m through the wide band B and neutral density 2 filters using the 5.2 arcsec pinhole. The star was chosen because it appears in the list of stars observed with the intensity interferometer at Narrabri [1]. The authors quoted a zero baseline correlation coefficient $C_N = 0.60 \pm 0.06$, very far from the value of 1 expected from a single unresolved star. Their explanation of the difference was that it is caused by the limited resolution of the stellar disk, which corresponds to an angular extent of the order of 0.5 mas for a uniformly illuminated disk. It is well known (see Ref [12] and [13]) that ζ Ori is a triple star, the secondary (ζ Ori B, V = 4.20, SpT =B0III, flux $B/A \approx 0.1$) being approximately 2.5 arcsec

distant to the South East, and therefore just at the edge of the used pinhole. The tertiary weaker component is too far to be of concern in our data.

With Iqueye, the photons collected by each SPAD arrive from four different sub-pupils: this allows us to consider the system as four parallel smaller telescopes, each focused on one SPAD. Clearly, the collecting area of each sub-aperture is small and the baseline distances d are fixed; therefore, we did not expect to obtain significant astrophysical results. Moreover, we expected $1 \geq G^{(2)}(d)_{\mathrm{NTT}} > G^{(2)}(0)_{\mathrm{NARR}} = C_N$. This expectation was motivated, first because the stellar disk cannot be resolved by the small baselines available with this setup, and second because the secondary star at the edge of the field of view should contribute a minimum amount of additional flux, since seeing occasionally scatters a fraction of its light outside the pinhole. Finally, because the maximum photon rate that can be handled with the present equipment is approximately 10 times lower than the minimum rate necessary to achieve an acceptable *S/N* ratio for detecting second order effects.

As already mentioned, during the whole observation, approximately 2×10^{10} photons were detected, and the time tags were collected in 7771 files each of 10 MB, for a total of 78 GB. Processing all these data with the smallest possible 24.41 ps coincidence windows lasted only three hours on a 32 GB RAM four processor machine.

To obtain a clearer understanding of the results and in particular to estimate the statistical errors affecting the determination of $G^{(2)}$, the entire string of 7771 files was divided into seven clusters of 1000 files each (the remaining 771 files were discarded), and the value of $G^{(2)}(d)$ was calculated for each cluster by setting a coincidence window Δt = 244.1 ps. From these values, the average $\langle G^{(2)}(d)\rangle$ was calculated together with its standard deviation. The results obtained from this analysis are summarized in Table 1.

Table 14: Values of $\langle G^{(2)}(d)\rangle$ obtained from one hour observation of the bright star ζ Ori, for each pair *a*, *b* of sub-apertures, assuming a time coincidence window Δt = 244.1 ps. The data set was divided in seven subsets, as explained in the text, and the reported values are the average of the seven obtained results.

Channel pair (channel numbers)	Effective distance d (m)	Resolving angle θ (arcsec)	$\langle G^{(2)}(d)\rangle$	Standard deviation
A-B	1.7	0.052	0.886	0.002
A-C	2.4	0.037	0.912	0.003
A-D	1.7	0.052	0.931	0.001
B-C	1.7	0.052	0.909	0.002
B-D	2.4	0.037	0.909	0.004
C-D	1.7	0.052	0.932	0.004

The table shows the pairs of SPADs used in the calculation, each SPAD being represented with a capital letter; not all combinations are shown because pairs A-B and B-A give identical results. The flux-weighted distance d between the two apertures is given in the second column, and the third column provides an indicative resolving angle computed as $\theta \approx \lambda/d$, where the

effective wavelength λ = 430 nm has been taken to be the center of the observing filter. The last two columns indicate the value of $<G^{(2)}(d)>$ and its standard deviation respectively. Note that the last column is not the true error in the value of $G^{(2)}(d)$, but simply the standard deviation of the average value $<G^{(2)}(d)>$, calculated by considering the seven independent 1000 file clusters.

It is clear that the algorithm is very stable, with relative fluctuations of $G^{(2)}(d)$ smaller than 1%. In addition, when all the 7771 files are processed together, the obtained $G^{(2)}(d)$ values differ from those of the 1000 clusters by less than 1%. Although the results are internally consistent, and even give values slightly less than 1 as a priori expected, we recall that this analysis was not designed to provide a true measurement, but simply to validate the method. The small aperture of the telescope and the already mentioned limitation in the dynamic range of the electronics , provided a signal-to-noise ratio too low to achieve significant astrophysical results. We therefore performed this experiment in preparation for an observation with two larger and more widely separated telescopes such as two VLTs or the two KECKs.

Nevertheless, we believe that these preliminary results are of sufficient interest to be expounded here because, to our knowledge, they represent the first attempt to perform intensity interferometry by time-tagging each detected photon and then post-processing the data, and thus avoiding real-time analog or digital correlators, which do not preserve data for all the original photon-events.

6. Conclusions and future plans

The main conclusions of our present study can be summarized as follows.

A new extremely fast photon-counting photometer, Iqueye, has been tested at NTT, where its superb potentiality for observing fast variable objects, such as pulsars, was clearly demonstrated. These tests permitted hours of uninterrupted observations with an absolute timing accuracy better than 0.5 ns. No failure or degradation has been encountered over two runs twelve months apart.

The results already obtained by Iqueye attest that a quantum photometer at the E-ELT will be able to measure second and higher order correlation functions, so opening the road to new tools of investigation of the Universe. Thus, Iqueye paves the way toward the realization of a truly “quantum” photometer for the 42 m E-ELT.

Iqueye2 has been left to the NTT ready for further observing runs. The controls have been moved to the newer general control room of the Observatory, so that the astronomer needs to go to the telescope only for the initial set-up.

Should resources permit, a third version (IT2) with two detecting heads will be built for two 8m telescopes of the VLT, in order to emphasize the HBTII scientific capabilities.

Iqueye can be upgraded in order to perform observations in larger instruments with multiple apertures such as the ESO VLTs and the KECKs, and in the future with subapertures of the E-ELT.

On the short term, Iqueye can be improved in several areas with existing technology and moderate resources. The maximum count rate can be increased: we are working, in conjunction with MPD on the optimization of the combination dead-time, after-pulsing and throughput of the NIM connector. CAEN can provide a dedicated TDC board having the acquisition computer

directly inside the VME crate. In this way, each SPAD of Iqueye should be able to raise the maximum data rate by at least a factor of four. The existing crate can be filled with 16 boards (6 are inserted at present), thus handling the pupil splitting of VLTs and KECKs. No great problem would be encountered by using a number of such electronic system to cope with the GigaHertz count rate produced by the E-ELT. Regarding the software correlator, a natural development is a version compatible with cluster computing facilities. The algorithm is highly parallelizable, since different machines can work independently with only a small amount of data sharing on different substrings of the main sequence.

On the longer term, when the E-ELT will actually be available, the technology would have evolved significantly beyond the contemporary one in all areas. In particular, photon counting multipixel arrays with good filling factors are likely to appear on the market, greatly easing the optical problem of coupling small size detectors to very large apertures.

Acknowledgements

Iqueye was constructed with funds provided by the Italian Ministry of University and Research, the University of Padova, and the National Institute for Astrophysics through the PRIN 2006 program; by the European Community through the Harrison Project for the scientific exploitation of the Galileo GNSS; and by Fondazione CARIPARO through the Project of Excellence 2006. The authors wish to express gratitude to ESO who granted technical time at NTT for the January 2009 run and covered part of the team travel expenses. Finally, a sincere acknowledgement is due to La Silla personnel, who participated very actively in the observational campaign and made a substantial contribution to the success of the instrument testing.

References

[1] D. Dravins, C. Barbieri, V. Da Deppo et al., *QuantEYE quantum optics instrumentation for astronomy. OWL Instrument Concept Study*, Tech. rep., ESO, Document OWL-CSR-ESO-00000-0162, 2005.

[2] C. Barbieri, G. Naletto, T. Occhipinti, C. Facchinetti, E. Verroi, E. Giro, A. Di Paola, S. Billotta, P. Zoccarato, P. Bolli, F. Tamburini, G. Bonanno, M. D'onofrio, S. Marchi, G. Anzolin, I. Capraro, F. Messina, M. Belluso, C. Pernechele, M. Zaccariotto, L. Zampieri, V. Da Deppo, S. Fornasier, F. Pedichini, *AquEYE, a single photon counting photometer for astronomy*, Journal of Modern Optics, **56**(2), 261-272, 2009.

[3] S. Cova, M. Ghioni, A. Lotito, I. Rech, F. Zappa, *Evolution and prospects for single-photon avalanche diodes and quenching circuits*, Journal of Modern Optics, **51**(9), 1267-1288, 2004.

[4] C. Barbieri, G. Naletto, I. Capraro, T. Occhipinti, E. Verroi, P. Zoccarato, C. Facchinetti, C. Germanà, M. Parrozzani, M. Zaccariotto, G. Anzolin, F. Tamburini, A. Di Paola, E. Giro, G. Bonanno, S. Billotta, C. Pernechele, P. Bolli, L. Zampieri, A. Possenti, A. Cadez, *Very fast photon counting photometers for astronomical applications: IquEYE for the ESO 3.5m New Technology Telescope*, SPIE Conference 7355B on Photon Counting Applications, paper number: 7355-25, Prague, 2009.

[5] G. Naletto, C. Barbieri, T. Occhipinti, I. Capraro, A. Di Paola, C. Facchinetti, E. Verroi, P. Zoccarato, G. Anzolin, M. Belluso, and 13 coauthors (2009): *Iqueye, a single photon-counting*

photometer applied to the ESO new technology telescope, Astronomy and Astrophysics, **508**(1), 531-539, 2009.

[6] S. Billotta, C. Barbieri, M. Belluso, G. Bonanno, G. Condorelli, S. Di Mauro, P.G. Fallica, P. Finocchiaro, M. Mazzillo, A. Pappalardo, D. Sanfilippo, C. Timpanaro, *Characterization of Detectors for the Italian Astronomical Quantum Photometer Project*, Journal of Modern Optics. **56**(2), 273-283, 2008.

[7] P. Zoccarato, C. Barbieri, T. Occhipinti, A. Cadez, D. Ponikvar, G. Naletto, I. Capraro, C. Cantelmo, *The importance of accurate timing of astronomical photons*, 2nd International Colloquium: Scientific and Fundamental Aspects of the Galileo Programme – COSPAR Colloquium, 14-16 October, Padua, Italy, 2009.

[8] T. Occhipinti, P. Zoccarato, I. Capraro, P. Bolli, F. Messina, G. Naletto, P. Villoresi, C. Barbieri, *The Importance of Time and Frequency Reference in Quantum Astronomy and Quantum Communications*, 39th Annual Precise Time and Time Interval (PTTI) Meeting, 26-29 November, Long Beach, California, USA, 2007.

[9] R. Hanbury Brown, *The intensity interferometer. Its applications to astronomy*, London: Taylor & Francis, 1974

[10] I. Capraro, G. Naletto, C. Barbieri, T. Occhipinti, E. Verroi, P. Zoccarato, S. Gradari, *Quantum Astronomy with Iqueye*, SPIE Conference Quantum Information and Computation VIII, paper number 7702-22, 2010.

[11] Capraro, G. Naletto, C. Barbieri, T. Occhipinti, E. Verroi, P. Zoccarato, A. Di Paola (2009), *A First attempt to Intensity Inetrferometry with IQUEYE*, Proceedings of 1 Quantum of Quasars workshop Grenoble, France December 2-4, 2009

[12] Barbieri C., Naletto G., Capraro I., Occhipinti T., Verroi E., Zoccarato P., Gradari S., Barbieri M., Germana' C., Zampieri L., Giro E., Da Deppo V., Di Paola A., Facchinetti C., Bolli P.,Pernechele C., Billotta S., Bonanno G., Messina F., Zaccariotto M. (2010) *Iqueye, a single photon counting very high speed photometer for the ESO 3.5m NTT***,** SPIE Conference "Advanced Photon Counting Techniques IV" invited paper 7681-4 Orlando Florida (USA) April 2010